J Physiol (2003), **553.2**, *pp.* 427–443

DOI: 10.1113/jphysiol.2003.051995
www.jphysiol.org

Journal of Physiology

Developmental shift from long-term depression to long-term potentiation in the rat medial vestibular nuclei: role of group I metabotropic glutamate receptors

Julien Puyal, Silvarosa Grassi*, Cristina Dieni *, Adele Frondaroli *, Danielle Demêmes, Jaqueline Raymond and Vito Enrico Pettorossi *

*INSERM U432, University of Montpellier II, Place Eugène Bataillon, F-34095 Montpellier Cedex 5, France and * Department of Internal Medicine, Section of Human Physiology, University of Perugia, Via del Giochetto, I-06100 Perugia, Italy*

The effects of high frequency stimulation (HFS) of the primary vestibular afferents on synaptic transmission in the ventral part of the medial vestibular nuclei (vMVN) were studied during postnatal development and compared with the changes in the expression of the group I metabotropic glutamate receptor (mGluR) subtypes, mGluR1 and mGluR5. During the first stages of development, HFS always induced a mGluR5- and $GABA_A$-dependent long-term depression (LTD) which did not require NMDA receptor and mGluR1 activation. The probability of inducing LTD decreased progressively throughout the development and it was zero at about the end of the second postnatal week. Conversely, long-term potentiation (LTP) appeared at the beginning of the second week and its occurrence increased to reach the adult value at the end of the third week. Of interest, the sudden change in the LTP frequency occurred at the time of eye opening, about the end of the second postnatal week. LTP depended on NMDA receptor and mGluR1 activation. In parallel with the modifications in synaptic plasticity, we observed that the expression patterns and localizations of mGluR5 and mGluR1 in the medial vestibular nuclei (MVN) changed during postnatal development. At the earlier stages the mGluR1 expression was minimal, then increased progressively. In contrast, mGluR5 expression was initially high, then decreased. While mGluR1 was exclusively localized in neuronal compartments and concentrated at the postsynaptic sites at all stages observed, mGluR5 was found mainly in neuronal compartments at immature stages, then preferentially in glial compartments at mature stages. These results provide the first evidence for a progressive change from LTD to LTP accompanied by a distinct maturation expression of mGluR1 and mGluR5 during the development of the MVN.

(Resubmitted 25 July 2003; accepted after revision 8 September 2003; first published online 12 September 2003)
Corresponding author S. Grassi: Department of Internal Medicine, Section of Human Physiology, University of Perugia, Via del Giochetto, I-06100 Perugia, Italy. Email: sgrassi@unipg.it

Adult vestibular glutamatergic synapses show long-term changes in their efficacy which can be induced in rat brainstem slices by high frequency stimulation (HFS) of the primary vestibular afferents (Capocchi *et al.* 1992; Grassi *et al.* 1996, Grassi & Pettorossi, 2001). In fact, HFS causes long-term potentiation (LTP) in the ventral part of the medial vestibular nuclei (vMVN) which is induced through the activation of *N*-methyl-D-aspartate (NMDA) receptors (Capocchi *et al.* 1992; Grassi *et al.* 1996, Grassi & Pettorossi, 2001) and requires group I metabotropic glutamate receptor (mGluR) activation for its consolidation (Grassi *et al.* 1998*b*, 1999, 2002). However, rat secondary vestibular neurons are immature at birth and show a progressive evolution of their morphological and electrophysiological characteristics leading to the typical adult responses only at the end of the first month (Lannou *et al.* 1979; Dutia *et al.* 1995; Johnston & Dutia, 1996; Dutia & Johnston, 1998; Murphy & Du Lac, 2001). In addition, the expression of AMPA and NMDA receptor subunits show notable modifications within vestibular nuclei (VN) during postnatal development (Sans *et al.* 2000). Because of these remarkable physiological and biochemical changes taking place in the vestibular neurons during the first month, it is conceivable that HFS-induced long-term effects may also vary during development, as occurs in other regions of rat brain where a shift from LTP to LTD, or vice versa, has been shown (Dudek & Bear, 1993; Battistin & Cherubini, 1994; Kirkwood *et al.* 1995; Lo & Mize, 2002). Such a change in plasticity might be important for the progressive synaptic development of vestibular neurons from birth to adulthood (Heywood *et al.* 1973; Karhunen, 1973).

The two subtypes of group I mGluRs, mGluR1 and mGluR5 (Conn & Pin, 1997), play a major role in facilitating or inhibiting LTP in the vMVN (Grassi *et al.*

2002). Consequently, we can expect that in the VN, together with changes in the expression of AMPA and NMDA receptor subunits (Sans *et al.* 2000), mGluR1 and mGluR5 expression may also vary with development and influence the long-term effect. Variations in the expressions and cellular distributions of mGluR1 and mGluR5 during postnatal development have been observed in other brain regions (Catania *et al.* 1994; Romano *et al.* 1996; Casabona *et al.* 1997) and implied in the control of neuronal events during development (Catania *et al.* 2001) when they could contribute, like the other glutamate receptors, to various physiological processes, including neuronal survival and synaptogenesis (Catania *et al.* 1994).

In this study we used electrophysiological and anatomical approaches to investigate the developmental changes of activity-dependent long-term effects and of the expressions and localizations of mGluR1 and mGluR5 in the rat vMVN. The aim of the electrophysiological experiments was to investigate, in brainstem slices during postnatal development, the effect of HFS of the primary vestibular afferent on the field potentials recorded in the vMVN. Antagonists for mGluR1, mGluR5 and NMDA receptors were used to elucidate the role of these receptors in the induction of the long-term effects of HFS in the vMVN. In parallel we investigated the expressions and distributions of mGluR1 and mGluR5 by non-radioactive *in situ* hybridization, immunoblotting and immunocytochemistry in rat vMVN at different stages of postnatal development. We analysed precisely whether the changes occurring in the temporal expression pattern of mGluR1 and mGluR5 during postnatal development of the vMVN were indicative of their putative roles in synaptic processing linked to modifications in the induction of the long-term effects of HFS.

METHODS

Animals

Rats (230 Wistar; 150 Sprague-Dawley) were used at various stages of postnatal (P) development from birth (P0) to adulthood (P28). The animals were used in accordance with the ethical guidelines of the Bioethical Committee of the University of Perugia (authorization number, 31/02) and the French Ministry of Agriculture and Forestry concerning animal care (authorization number, 04889).

Chemicals

Drugs used were all purchased from Tocris Cookson (Bristol, UK) and included: the non-competitive mGluR1 antagonist, 7-(hydroxyimino)cyclopropa[b]chromen-1a-carboxylate ethyl ester (CPCCOEt, 125 μM) (Litschig *et al.* 1999), the non-competitive mGluR5 antagonist, 2-methyl-6-phenylethynyl-pyridine (MPEP, 20 μM) (Gasparini *et al.* 1999), the antagonist for $GABA_A$ receptors, (−)-bicuculline methochloride (20 μM), the antagonist for NMDA receptors, D, L-2-amino 5-phosphono-pentanoic acid (AP-5, 100 μM) and the AMPA receptor antagonist, 6-cyano-7-nitroquinoxaline-2, 3-dione (CNQX, 10 μM). The drug concentrations were those used in our previous study (Grassi *et al.* 2002).

Stock solutions of MPEP, AP-5, bicuculline and CNQX (10 mM) were prepared in distilled water, and CPCCOEt (5 mM) was prepared in 2% dimethylsulphoxide (DMSO). As previously reported (Grassi *et al.* 1998*a*), DMSO at the final concentration (0.05%), had no effect on baseline potentials and LTP induction. Drug solutions were freshly prepared in artificial cerebrospinal fluid (ACSF) and perfused at a rate of 2 ml min^{-1}. The ACSF contained (mM): NaCl 124, KCl 3, KH_2PO_4 1.25, $NaHCO_3$ 26, $CaCl_2$ 3.4, $MgSO_4$ 2.5, D-Glucose 10 and L-ascorbate 2.

Each drug was infused for 10–15 min and HFS was applied 5–10 min after the arrival of the drug in the recording chamber. Our previous studies demonstrate that in our experimental system the drugs used are completely washed out 15–20 min after the end of infusion (Capocchi *et al.* 1992, Grassi *et al.* 1995, 2002).

Slice preparation

The experiments were performed on 506 brainstem slices obtained from Wistar rats (Harlan-Nossan, Italy) at P6–P28. Under anaesthesia with ether, the animals were decapitated, and the cranium opened to expose the entire brain. The methods for preparing and maintaining the slices have been reported previously (Capocchi *et al.* 1992; Grassi *et al.* 1995). In brief, transverse 400 μm thick slices containing the MVN were incubated in warmed (30–31 °C) oxygenated ACSF, and transferred after 1 h to an interface-type recording chamber and perfused at a rate of 2 ml min^{-1}.

Electrophysiological recording and stimulating technique

The field potentials elicited by vestibular afferent stimulation were recorded in the ventral part of the MVN (vMVN) with 2 M sodium chloride-filled micropipettes (resistance, 3–10 MΩ) (Fig. 1). The recorded field potentials consisted of a large negative (N1) wave, which followed the artefact and represented the monosynaptic activation of the secondary vestibular neurons (Fig. 1*B* and *C*). Usually, the field potentials were similar to those recorded in the adult animals, but they were evoked by lower stimulus intensity. As reported previously (Grassi *et al.* 1996), the postsynaptic nature of the N1 wave was verified by a 3 ms interval paired-pulse test, which caused the disappearance of the N1 wave (Fig. 1*C*), and by using a Ca^{2+}-free solution (not shown). The dependence of this field potential on AMPA receptor activation was verified by using the AMPA antagonist CNQX, which caused the disappearance of the N1 wave 7.5 min after the start of drug infusion (Fig. 1*B* and D). The effect of CNQX was reversible, as the N1 wave recovered its control amplitude about 15–20 min after removal of the drug from the bath (Fig. 1*D*). The recorded potentials were amplified, filtered with a wideband filter (0–10 kHz) and stored in a computer equipped with a data acquisition card (AT-MIO-16E-2, National Instruments, Austin, TX, USA).

One bipolar NiCr-stimulating electrode was placed at the point where the vestibular afferents enter the MVN, which is in a narrow zone at the medial border of the lateral or descending vestibular nucleus (Fig. 1*A*). The distance between stimulating and recording electrodes was about 1 mm. We did not use more lateral positions, because, as previously reported (Grassi *et al.* 1999, Grassi & Pettorossi, 2000), the probability of eliciting field potentials was very low when the stimulating distance increased. However, our previous studies show no difference in the results between medial and lateral stimulation. In addition, in all our previous studies we were never able to evoke any measurable potential when the stimulating electrode was placed outside the

loci where the vestibular afferents were probably localized and, in some cases, clearly visible. This was also confirmed by histological examination. This also rules out the possibility that the elicited responses are due to activation of fibres mediating internuclear interaction. Stimulus test parameters were: intensity, 20–100 μA; duration, 0.07 ms; and frequency, 0.06 Hz. We adjusted stimulus intensity so that the amplitude of N1 wave was 40–60 % of the maximum as determined by an input–output curve. HFS consisted of four bursts at 100 Hz applied with alternated polarity for 2 s with a 5 s interval. In all our previous studies, in adult rats, we have shown that HFS induces LTP in the vMVN in about 70–75 % of the cases, and has no effect in the remaining cases. It has been shown that higher or lower frequencies are less efficacious (Grassi *et al.* 1996). We used bursts at 100 Hz to mimic over-activation that could occur in the primary vestibular afferents in response to high velocity head rotation in the adult rats. The same frequency of stimulation has been applied in younger rats in order to describe the occurrence of LTP during development. However, 100 Hz burst activity is less probable in primary vestibular afferents of young rats. In fact, the spontaneous discharge of the primary neurons is rather low, even if the increase in spike frequency in response to natural stimulus is, after postnatal day 6, similar to that of the adult (Curthoys, 1982). Therefore, we tested lower frequencies (10, 20 and 50 Hz) in young animals (P8 and P10). Since we found no difference in the probability of obtaining LTD or LTP in these rats, we only reported the results obtained by using 100 Hz. In addition, we also excluded a possible failure of the afferent fibres to follow HFS at 100 Hz in very young rats since the field potential P wave, which represents the afferent volley, was unchanged during and after HFS.

The recording and stimulating sites were marked, in each slice, by passing DC current of 50–100 μA for 10–20 s and subsequently verified by histological analysis.

Data collection

We measured the amplitude of the N1 wave as the difference between the wave peak negative voltage and a baseline influenced by the electrical stimulus decay (Fig. 1*C*). To quantify this voltage decay, responses to the 3 ms interval paired-pulse test were recorded before and after application of both drug and HFS, as the second response of the paired-pulse stimulation represented only the electrical stimulus. To show the different effects of HFS on N1 amplitude during postnatal development (P6–P21) we calculated the percentage occurrence of LTP, LTD and null effects (NE) in all the slices stimulated at each age (10–35 slices from 5–15 animals). The effect of HFS was also analysed in slices from rats at P26–P28 (6 slices from 3 animals, for each age) which can be considered adult rats. The effect of HFS in the presence of AP-5, MPEP, bicuculline or CPCCOEt was analysed in 6 slices (3 animals) for each age. The wave amplitudes were measured every 15 s and expressed as a percentage of the baseline (the mean of the responses recorded within the first 5 min of each experiment). To compare the effects within a single experiment and among different ones, we considered the average value and S.D. within a 5 min interval at the steady state of each experimental condition. In each experiment the differences between the values were evaluated using analysis of variance (ANOVA) and Tukey's *post hoc* test. Statistical significance was established at $P < 0.05$.

Because LTP induced by HFS at different ages showed different time courses, we also calculated the rise time of LTP as the time (min) from HFS necessary to reach the potentiation steady state. The values are obtained from three consecutive age groups.

Non-radioactive *in situ* hybridization procedure

The labelled mGluR1 and mGluR5 probes were used to determine the cellular distribution of mGluR1 and mGluR5 mRNA in the vMVN of brainstem cryostat sections obtained from P6 and P21 Sprague-Dawley rats. The sections were selected from the rat brain atlas (Paxinos & Watson, 1986) in the central level of the VN (Figs 1*A* and 5*A*). We used cytoarchitectural criteria derived from those of Mehler & Rubertone (1985) on alternate cresyl violet-stained sections, to define the borders of the VN subdivisions. The hybridization procedure used has been described elsewhere (Puyal *et al.* 2002) and was performed using 3′ end digoxigenin-labelled oligonucleotide antisense probes (45 bases long) complementary to the rat mGluR1 mRNA (sequence 5′-GGA GCG GAA GGA AGA AGA TCC ATC TAC ACA GCG TAC CAA ACC TTC-3′, corresponding to amino acids 484–498) and rat mGluR5 mRNA (sequence 5′-GCA GCG GAA GGA AGA AGA TCC ATC ATC TAC ACA GCG TAC TAC CAA ACC TTC-3′, corresponding to amino acids 124–138) previously used by Fotuhi *et al.* (1994). For each labelled probe the control sections were hybridized in the presence of 10-fold excess of unlabelled probe. Excess unlabelled probe was added during hybridization to check that hybridization was specific. No hybridization signal was detected under these conditions. Omission of the labelled probe from the hybridization buffer or incubating the slides with the colour detection buffer alone resulted in no detectable cell staining.

Western blot analysis

Three rats were used for each postnatal stage P0, P7, P14, P21 and P28. After decapitation under anaesthesia with Nembutal (30 mg kg^{-1}) the brainstem was dissected out and the cerebellum removed. Under the microscope, coronal brainstem slices (200–300 μm thick) containing the rostro-caudal extent of the VN were cut. VN, located within the sections by anatomical landmarks and position with respect to the fourth ventricle, were rapidly dissected out. Each sample contained the MVN, the lateral vestibular nuclei (LVN), the descending vestibular nucleus, small amounts of the medial longitudinal fasciculus and the superior VN. Vestibular tissues were homogenized in a homogenization buffer (2 mM EDTA, 10 % glycerol, 2.3 % SDS, 62 mM Tris pH 6.8 and a protease inhibitor cocktail from Boehringer). The resulting lysates were boiled for 5 min, centrifuged and protein concentration was determined by using a protein assay reagent BCA (Pierce, Rockford, IL, USA) and by measuring the absorbance at 562 nm on a microplate reader (Dynatech PC software). SDS-PAGE (12.5 % acrylamide gel) was performed in a mini-protease II dual slab-cell apparatus (Biorad Laboratories, Hercules, CA, USA). Each extract (30 μg per lane) was then subjected to electrophoresis and electroblotted onto a nitrocellulose membrane (Hybond ECL, Boehringer Mannheim). Transfers were performed overnight in 20 mM Tris, 150 mM glycine, 20 % methanol buffer and 0.01 % SDS. Membranes were blocked, for 1 h, in Tris-buffered saline (TBS) containing 8 % non-fat milk powder and then were probed with rabbit antibody directed against mGluR1 (1:300, Chemicon) or rabbit antibody directed against mGluR5 (1:300, Chemicon, Temecula, USA), diluted in 5 % bovine serum albumin (BSA) in TBS. After washing in TBS and 0.2 % Tween-20 blots were incubated with peroxidase-conjugated goat anti-rabbit IgG (1:750, Jackson ImmunoResearch Laboratories, West Grove, PA, USA) for 1 h at room temperature. Antigen–antibody complexes were visualized by enhanced chemiluminescence (ECL)(Amersham). Molecular sizes were estimated by separating prestained molecular mass markers (219 to 8800 Da) in parallel (Kaleidoscope, Biorad

Laboratories, CA, USA). Protein bands of interest were analysed by measuring optical density (OD) by scanning densitometry, as previously described (Puyal *et al.* 2002). Densitometric analyses of these bands were carried out at the various stages and the OD of mGluR1α or mGluR5 for each stage was expressed in terms of arbitrary units of band intensity × band area. The relative levels of mGluR1α and mGluR5 were normalized as a percentage of the P28 value for mGluR1α and mGluR5, respectively, and compared using Student's *t* test to assess the significant ($P < 0.05$) differences between the various postnatal stages. The means of mGluR1α and mGluR5 levels from each postnatal stage were reported ± S.E.M. The Western blots presented are typical of five similar experiments.

Light microscopic immunocytochemistry

Rats from P0, P7, P14, P21 and P28 ($n = 3$ to 5 for each stage) were anaesthetized with Nembutal (30 mg kg^{-1}, intraperitoneally) and transcardially perfused with an ice-cold solution containing either 4 % paraformaldehyde in 0.1 M phosphate-buffered saline (PBS, pH 7.4) or 4 % paraformaldehyde supplemented with 0.25 % glutaraldehyde for electron microscopy immunocytochemistry. The brainstem and cerebellum were rapidly dissected and postfixed in the same fixative for 10 h at 4 °C. The samples were immersed overnight in 30 % sucrose in 0.1 M PBS at 4 °C. Subsequently 14 μm-thick coronal sections were cut on a freezing microtome and collected on polylysine-coated slides. Immunofluorescence detection was carried out as described earlier (Puyal *et al.* 2002). The sections were pre-incubated in 10 % donkey serum diluted in PBS and 0.3 % Triton-X 100 for 30 min, then incubated overnight at room temperature with the primary antibodies. The antibodies used and their dilutions in PBS containing 1 % donkey serum and 0.1 % Triton X-100 were: anti-NF 70 kDa mouse monoclonal antibody (Chemicon), 1:400; anti-mGluR1α rabbit polyclonal antibody (Chemicon), 1:300; anti-mGluR5 rabbit polyclonal antibody (Chemicon), 1:300; anti-GFAP mouse monoclonal antibody (Chemicon), 1:200; anti-synaptophysin mouse monoclonal antibody (Synaptic Systems, Göttingen, Germany), 1: 200. After washing in PBS, the sections were incubated for 90 min with fluorescein isothiocyanate (FITC)-conjugated donkey anti-rabbit IgG, or Texas Red-conjugated donkey anti-mouse IgG (diluted 1:200; Jackson ImmunoResearch, PA, USA).They were thoroughly rinsed in PBS and mounted in FluorSave (Calbiochem, San Diego, CA, USA).

For the double-labelling, the sections were incubated with the following mixtures of primary antibodies: mGluR/NF, mGluR/GFAP and mGluR/Synaptophysin, then with a mixture of FITC-labelled anti-rabbit IgGs and Texas Red-labelled anti-mouse IgGs, both diluted 1:200 in PBS. The samples were examined with a Biorad MRC-1024 laser scanning confocal microscope. For double-labelling, immunoreactive signals were sequentially visualized in the same section with two distinct filters, with acquisition performed in separated mode. Control sections were incubated in the absence of primary antibodies. No specific immunofluorescence was detected for any of these controls.

Electron microscopic immunocytochemistry by pre-embedding immunoperoxidase method

After perfusion, as described above, the brainstem blocks from P6 and P21 ($n = 5$, for each stage) were postfixed overnight in a fixative solution without glutaraldehyde then washed thoroughly for 3 h in PBS. Sections (68 μm thick) were cut on a vibratome and collected serially in cold 0.1 M PBS. Free-floating sections were cryoprotected with 25 % sucrose and 10 % glycerol for 2 h, quickly frozen in liquid nitrogen and thawed in 0.1 M PBS. They were incubated for 1 h in 10 % goat serum diluted in PBS. Sections were then transferred into the primary antibodies, diluted as mentioned above in the presence or absence of 0.05 % Triton X-100, at 4 °C with gentle agitation, for 40 h. After washing in PBS, the sections were incubated for 150 min in biotinylated goat anti-rabbit IgG (1:500, Vectastain Elite Kit, Vestor Laboratories, Burlingame, CA, USA) and in ABC reagent (1:100) for 2 h. Peroxidase enzyme activity was revealed by a 8–10 min incubation in 0.06 % 3, 3′-diaminobenzidine and 0.02 % H_2O_2 in 0.1 M PBS (pH 7.4). After the peroxidase reaction, the sections were transferred to distilled water and small parts of the ventral portion of the MVN were microdissected out. Samples were osmicated in 1 % OsO_4 in PBS for 30 min, dehydrated and embedded in Araldite 502/Embed 812 kit (Electron Microscopy Sciences, Washington, PA, USA). Ultrathin sections were contrasted with aqueous uranyl acetate followed by lead citrate and examined in a Jeol JEM 1200 transmission electron microscope.

RESULTS

Effect of HFS on the field potentials elicited in the vMVN during postnatal development

We examined the effect of HFS on the field potential N1 wave in slices from developing rats (P6–P21), and from adult rats (P26–P28) (Fig. 2*C*). From P6 to P13, HFS induced a significant reduction of the N1 amplitude, which began 5 min after HFS and reached a steady state about 5–10 min later (Fig. 2*A*). The persistence of depression throughout the recording period (> 60 min) allows us to consider it as a long-term effect (Fig. 2*A*). The HFS-dependent depression was similar in all ages and the N1 amplitude was reduced to 80.06 ± 5.07 % ($n = 30$) of the control. At P6 ($n = 13$) HFS induced LTD in 85 % of the examined cases, while it had no effect in the other cases (Fig. 2*C*). The probability of inducing LTD progressively decreased and LTD was no longer observed after P13 (Fig. 2*C*). The reduction of the occurrence of LTD with age was accompanied by an increase in the probability of LTP and null effect (NE) (Fig. 2*C*). In fact, at P7 ($n = 14$) LTP and NE were obtained in 7 % and 22 % of the examined cases, respectively, while at P10 ($n = 11$) LTP occurred in 37 % of the cases and NE in 40 % of the cases. At P11–P12, the percentage of LTP remained stable, while that of NE increased. Then, at P13–P15 ($n = 87$) the probability of inducing LTP suddenly increased to 65 % of the cases with a decrease in NE, and it reached 70–75 % at P17–P21 ($n = 63$) (Fig. 2*C*), a percentage very similar to that observed at P26–P28 ($n = 18$) (Fig. 2*C*) and at the adult stage in all our previous studies (Capocchi *et al.* 1992; Grassi *et al.* 1996, 1998*a*,*b*, 1999, 2002; Grassi & Pettorossi, 2000, 2001).

As far as the features of LTP are concerned, the amplitude of LTP was rather constant throughout development until the adult stage (131.19 ± 8.53 % of the control, $n = 131$) and it was not statistically different compared with that observed in the adult animals. By contrast, the rise time of LTP progressively decreased from P7 to the adult stages

and it was 15 ± 2.97 min (n = 10) in slices from P7–P9, 5.32 ± 0.55 min (n = 35) at P16–P18 and 2.95 ± 0.34 min (n = 24) at P19–P21 a value close to that observed in the adult (2.75 ± 0.56 min, n = 12, P26–P28) (Fig. 2*B* and 5B).

Dependence of LTD and LTP on NMDA receptors

The dependence on NMDA receptor activation of LTD and LTP induced by HFS during the development was assessed by using the NMDA antagonist (AP-5). In the presence of AP-5, HFS only induced LTD, which persisted after washout, while, like in the adult, LTP never occurred (Fig. 3*A*). The N1 amplitude was reduced by HFS in the presence of AP-5 to 75.81 ± 6.85 % (n = 35), a value which was not significantly different when compared with that obtained after HFS alone, but LTD appeared more frequently compared with the untreated slices, and it was still inducible until P17 (Fig. 3*A*). In fact, LTD occurred in 100 % of the cases at P6–P9 (n = 24) (Fig. 3*A*), in 50 % of the cases at P10 (n = 6) and in 33 % of the cases at P11–P16 (n = 24) (Fig. 3*A*).

Dependence of LTD and LTP on mGluR1 and mGluR5

We also analysed the role of the subtypes of group I mGluRs, mGluR5 and mGluR1, in LTP and LTD during development, by testing the effects of HFS in the presence of non-competitive antagonists for mGluR5 (MPEP) and for mGluR1 (CPCCOEt).

During development, MPEP did not modify the field potential amplitude under basal conditions, but, it prevented LTD induced by HFS in slices from P6–P13 rats (n = 36) (Fig. 3*B*). By contrast, the probability of inducing

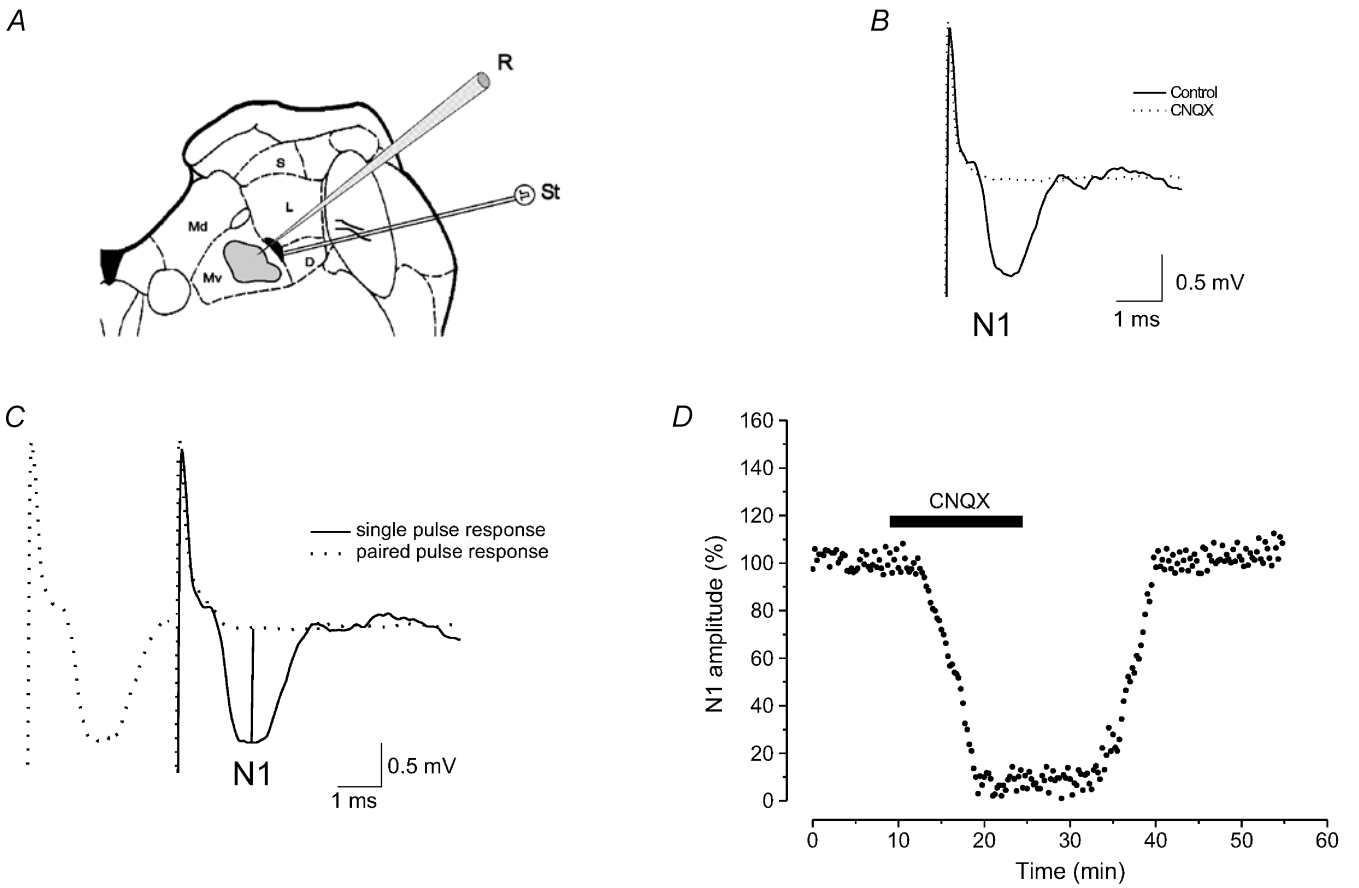

Figure 1. Recordings in the ventral part of the MVN

A, diagram of a brainstem slice showing the zone (shaded area) in the vMVN where recordings were performed and the stimulating loci (black area). *B*, typical vestibular field potentials recorded in the vMVN before and during infusion of the AMPA receptor antagonist, CNQX. *C*, single pulse response is superimposed onto a 3-ms paired pulse stimulation to show how peak N1 negative voltage was calculated compared to the baseline (vertical lines). *D*, effect of CNQX on the amplitude of field potential N1 wave. In this and in the following figures, the N1 wave amplitude was measured every 15 s, expressed as a percentage of the baseline and plotted as a function of time in a single experiment (time course). The bar shows the CNQX infusion period. Note the reversible abolition of N1 wave provoked by CNQX. D, descending vestibular nucleus; Md, dorsal part of the medial vestibular nucleus; Mv, ventral part of the medial vestibular nucleus; L, lateral vestibular nucleus; S, superior vestibular nucleus; R, recording electrode; St, stimulating electrode.

LTP at these ages increased compared with that of untreated slices (Fig. 3*B*), and, unlike LTP induced by HFS alone, LTP evoked in the presence of MPEP showed a rise time which was not statistically different from that observed in the adult state (Fig. 5*A* and 5B). From P14 to P18 ($n = 30$), HFS in the presence of MPEP induced LTP with a probability very similar to that observed after HFS alone (Fig. 3*B*). In slices after P18, administration of MPEP was able to induce LTP, like in the adult rats (Grassi *et al.* 2002).

We also investigated, during development, the effect of HFS in the presence of CPCCOEt, the antagonist for mGluR1. CPCCOEt, applied in slices during development, completely prevented LTP at any age (Fig. 3*C*), while in the presence of CPCCOEt, the probability of inducing LTD increased and the depression of the N1 wave (78.45 ± 6.33 %, $n = 33$) could be still observed at P17 in 33 % of the cases (Fig. 3*C*). At P11–P13, HFS following administration of CPCCOEt induced a slight potentiation in four cases (114.93 ± 7.34 %, $n = 4$) which quickly disappeared on washout in all the cases. After P19, HFS in the presence of CPCCOEt induced a potentiation showing a time course, after washout, like that observed in the adult animals. In fact, at P19–P21 ($n = 18$) and P26–P28 ($n = 18$), HFS following application of CPCCOEt induced a slight potentiation (116.98 ± 3.35 %, $n = 24$) which fully developed at drug washout (138.12 ± 4.72 %, $n = 24$).

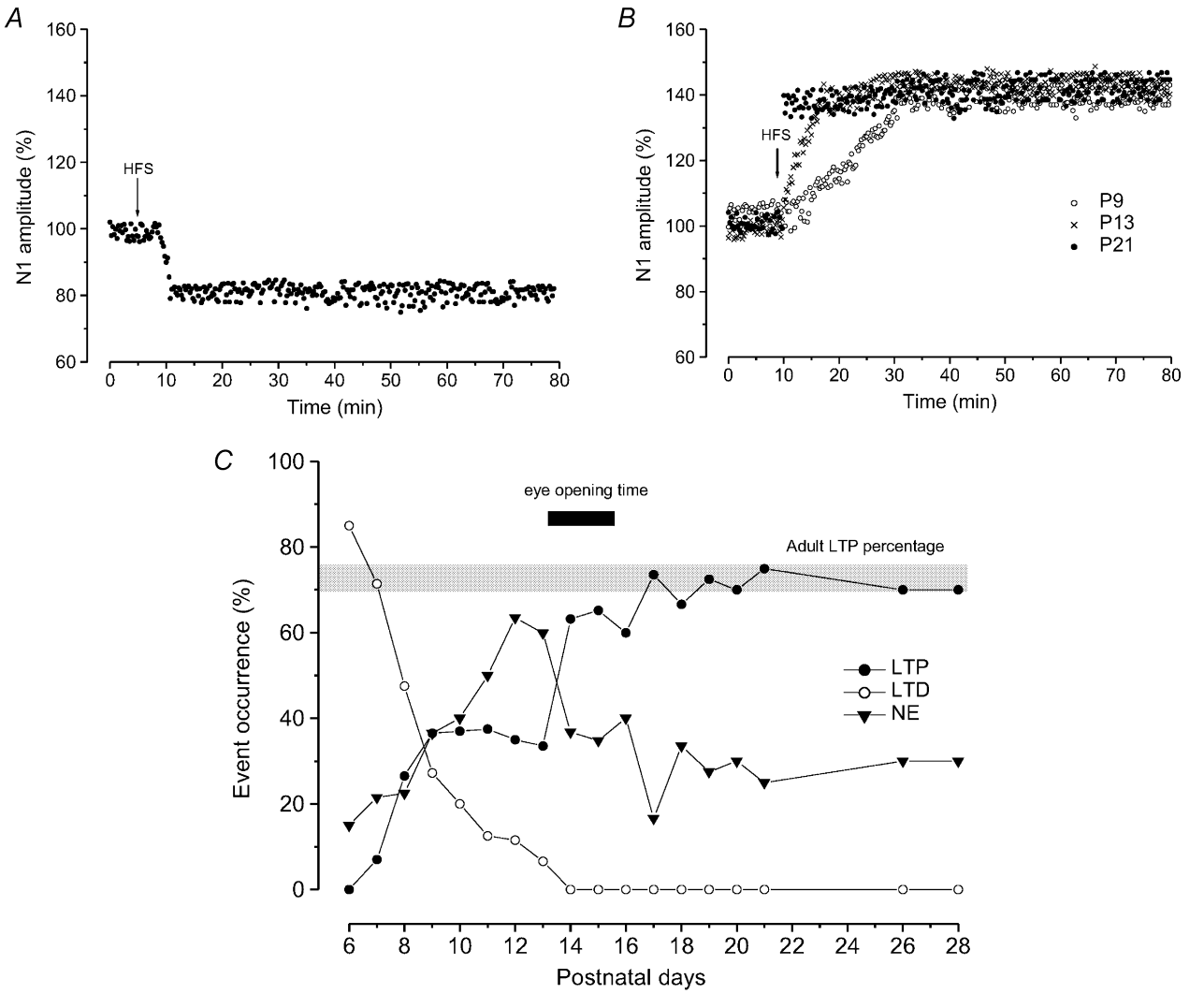

Figure 2. LTD and LTP induced by HFS in the vMVN during postnatal development

A and *B*, time courses of effects of HFS; the arrows show the time of delivery of HFS. *A*, typical time course of LTD induced by HFS from P6–P13. *B*, time courses of LTP induced by HFS at P9 (○), P13 (×) and P21 (●). Note the gradual increase of N1 amplitude after HFS at P9 and P13. *C*, each point in the graph represents the percentage occurrence of LTP (●), LTD (○) and NE (▼) after HFS in different age groups (the slice number for each group is reported in the Methods). The grey bar indicates the percentage occurrence of LTP observed in the adult (70–75 %). Note the abrupt change in occurrence of LTP at the time of eye opening (black bar).

To ensure that LTP induced by HFS in the presence of MPEP and LTD induced by HFS in the presence of CPCCOEt were truly due to the interference of mGluR5 and mGluR1 block with long-lasting synaptic events and not to a permanent binding of the antagonists, we delivered HFS after the end of the MPEP or CPCCOEt infusion. HFS delivered 15 min after the end of drug infusion, was able to induce LTD after MPEP administration (4 out of 5 slices at P7) and LTP after CPCCOEt administration (3 out of 5 slices at P10), demonstrating washout of the drug at this time.

Dependence of LTD on $GABA_A$ receptors

We also investigated the possible involvement of inhibitory GABAergic interneurons in the HFS-induced LTD and LTP, by analysing the effect of HFS in the presence of bicuculline, the antagonist for $GABA_A$ receptors, in P7–P10 ($n = 24$) and P21 ($n = 6$) slices. Bicuculline did not modify the field potential amplitude under basal conditions in all the examined cases, but it always prevented LTD induced by HFS in P7–P10 slices (Fig. 4*A* and *B*). In fact, HFS in the presence of bicuculline, only caused LTP ($n = 11$) or null effect ($n = 13$) (Fig. 4*A*

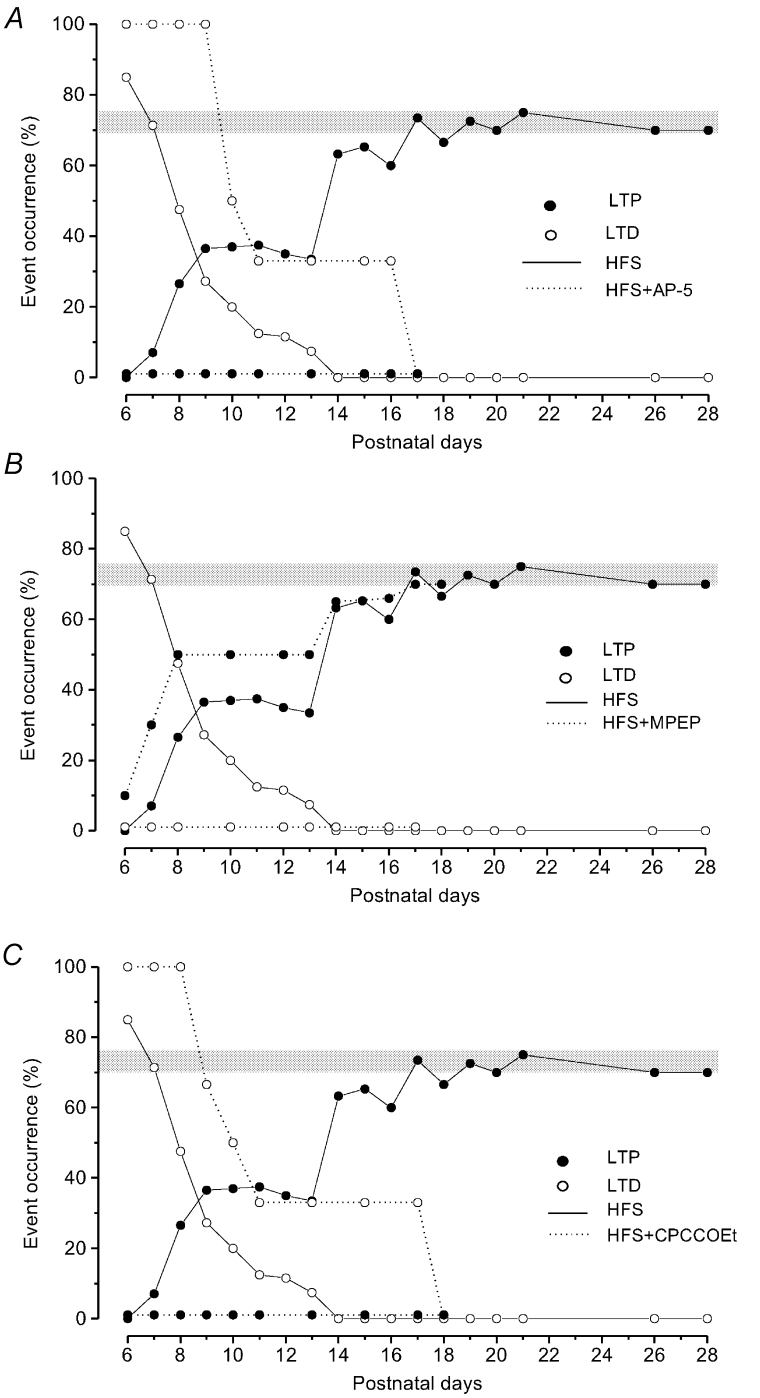

Figure 3. Effect of block of mGluR5, mGluR1 and NMDA receptors on the induction of LTD and LTP by HFS during postnatal development

Occurrence (%) of LTD (○) and LTP (●) during postnatal development in normal conditions (HFS alone, solid lines) and under receptor block (HFS + receptor antagonist, dotted lines). The grey bars indicate the percentage of LTP occurrence in the adult (70–75 %). *A*, effect of NMDA receptor block (AP-5). Note the increase of LTD and the complete disappearance of LTP, *B*, effect of mGluR5 block (MPEP). Note that in the presence of MPEP, LTD is completely prevented and the LTP occurrence increases. *C*, effect of mGluR1 block (CPCCOEt). Note that as with AP-5, CPCCOEt completely prevents LTP and unmasks LTD.

and *B*). By contrast bicuculline did not interfere with the effect of HFS at P21 (Fig. 4*B*).

In other P7–P10 ($n = 24$) slices, HFS was also delivered during the simultaneous application of bicuculline and MPEP. In this condition, HFS provoked the same effect as in the presence of bicuculline or MPEP alone, that is, LTP ($n = 11$) or null effect ($n = 13$), respectively.

To verify whether inhibitory GABAergic interneurons were responsible for the maintenance of HFS-induced LTD we also administered bicuculline after the induction of LTD in P7 slices ($n = 5$). In all these cases, bicuculline did not affect the depression induced by HFS (Fig. 4*A*).

Cellular distribution of mGluR1 and mGluR5 mRNAs in the vMVN during postnatal development

In situ hybridization analysis with the oligonucleotide probes recognizing mGluR1 and mGluR5 mRNA was performed in the vMVN (Fig. 6*A*) at two stages of development (P6 and P21). mGluR1 and mGluR5 mRNA

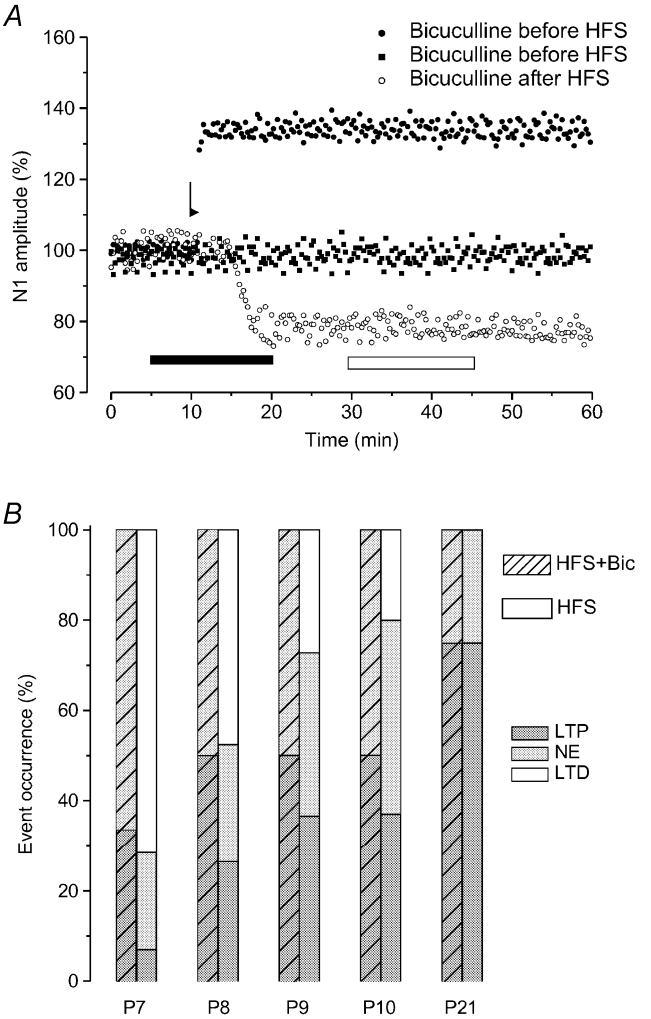

Figure 4. Effect of $GABA_A$ receptor block (bicuculline) on LTD induced by HFS at the early stage of development

A, time courses of the effects of bicuculline applied before (● and ■) and after (○) HFS in different experiments at P8. Note that in the presence of bicuculline, HFS only induces LTP (●) or null effect (■), while bicuculline applied after HFS, when depression is induced has no effect. The arrow shows the time of delivery of HFS, and the bars show the infusion period of bicuculline before HFS (■) and after HFS (□). *B*, percentage occurrence of LTP (dark grey bar), null effect (light grey bar) and LTD (open bar) after HFS applied alone (□) and during bicuculline infusion (▨) in P7–P10 and P21 slices.

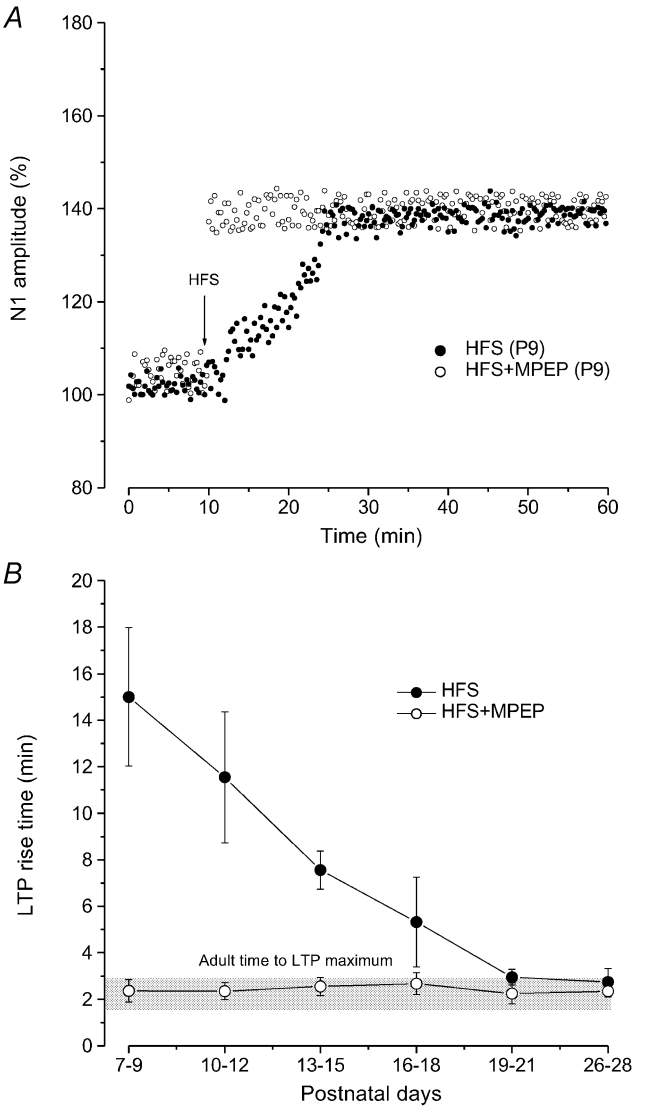

Figure 5. Effect of mGluR5 block (MPEP) on the rise time of LTP induced by HFS during postnatal development

A, time courses of LTP induced by HFS at P9 in untreated slices (●) and under MPEP (○). The arrow indicates the time of delivering HFS. Note the consistent reduction of rise time when LTP is induced in the presence of MPEP. *B*, plot showing the rise time of LTP induced by HFS at different ages in untreated slices (●) and in the presence of MPEP (○). Each point represents the mean ± S.D. of LTP rise time (min) evaluated by pooling all the values obtained from three consecutive age groups. Note that following application of MPEP the LTP rise time is similar to that observed in the adult (grey bar) at all the examined ages.

showed a different expression pattern in the developing vMVN. For mGluR1 mRNA, at P6, the staining was extremely weak or absent (Fig. 6*B*). At a later stage (P21), more than 90 % of vMVN neurons presented a strong level of mGluR1 mRNA expression (Fig. 6*C*). For mGluR5 mRNA, at P6, numerous vMVN neurons were strongly labelled and a faint labelling was detected between them (Fig. 6*D*). At later stages (P21), the number of mGluR5-labelled neurons decreased appreciably (Fig. 6*E*).

Western blot analysis of mGluR1 and mGluR5 proteins in the VN of developing rats

The presence and relative amounts of mGluR1α and mGluR5 proteins were assessed by Western blot analysis using anti-mGluR1α and anti-mGluR5 antibodies. At different stages of rat development, the protein extracts were obtained from the total microdissected VN (Fig. 7). Immunoblots of mGluR1α (Fig. 7*A*) showed an immunoreactive band around 142 kDa corresponding to its predicted size (Reid *et al.* 1995). Immunoblot of mGluR5 (Fig. 7*C*) showed an immunoreactive band around 148 kDa corresponding to its predicted size (Romano *et al.* 1995). The temporal expression patterns differed for the two proteins. Densitometric analysis of mGluR1α band intensity (Fig. 7*B*) indicated that although detectable at birth, the signal intensity remained very low during the first week, then increased to a high level at the end of the third week (P21) and remained similarly high at P28. Unlike mGluR1α, densitometric analysis of mGluR5 band intensity (Fig. 7*D*) indicated a very high level of expression at birth, which remained stable during the first week, and then decreased strongly from P14 to P21, to reach a very low level at mature stages (P28).

Distribution patterns of immunoreactivities for mGluR1α and mGluR5 in the vMVN during postnatal development

mGluR1α and mGluR5 protein expressions were examined in the vMVN from birth to P28 using immunocytochemistry visualized with confocal and electron microscopy.

mGluR1α. During the first week of development, the mGluR1α immunoreactivity density was very low (Fig. 8*A* and *C*) and light staining was found in few neuronal cell

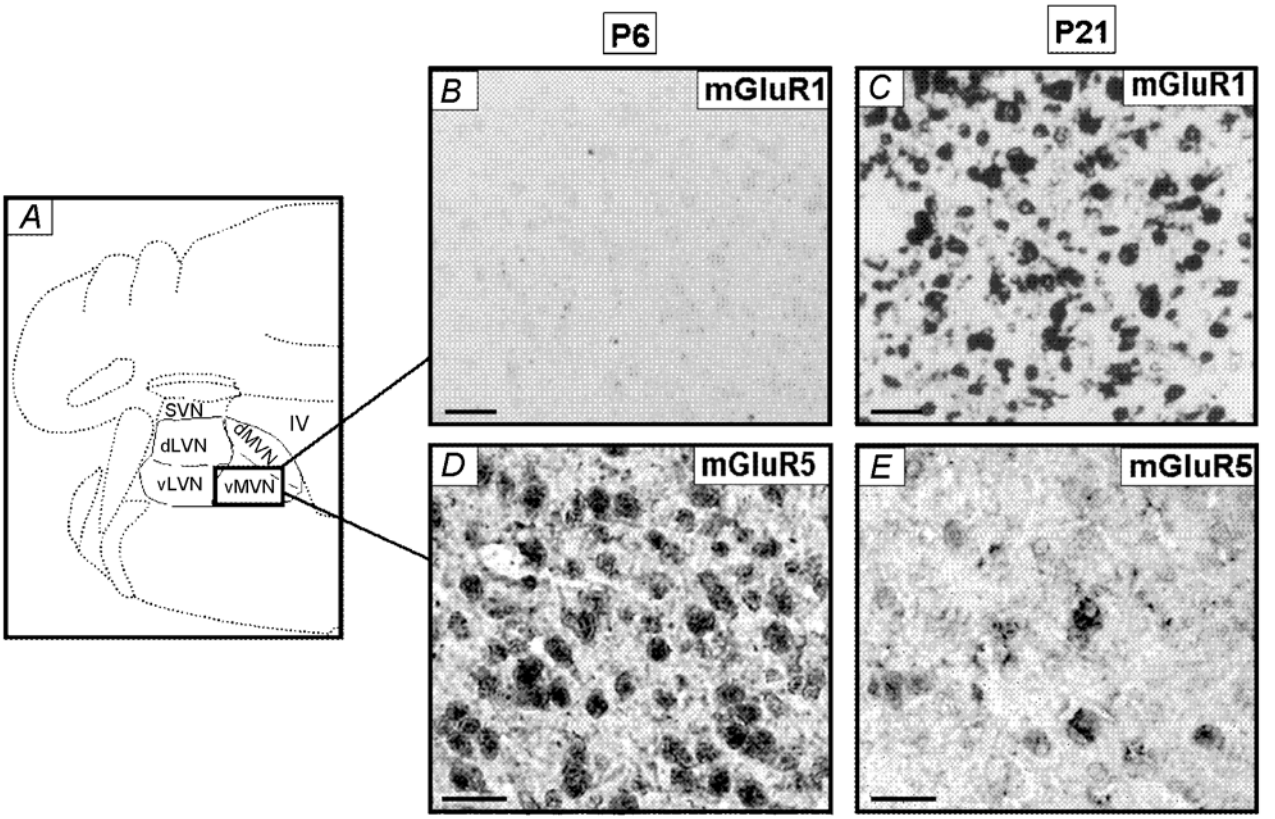

Figure 6. Distribution of hybridization signals for mGluR1α and mGluR5 mRNA in the rat MVN during postnatal development

A, schematic representation of the various regions of the VN on adult coronal section of the brainstem. vMVN, ventral part of the MVN; dMVN, dorsal part of the MVN; dLVN, dorsal part of the LVN; vLVN, ventral part of the LVN; SVN, superior VN; IV, fourth ventricle. *B–E*, brainstem sections at different postnatal (P) days were hybridized using specific oligoprobe for mGluR1 (*B* and *C*) and mGluR5 (*D* and *E*). Scale bars, 25 μm.

bodies (Fig. 8*C*). In addition, rare thin-labelled profiles were detected. From the second week, the density of immunoreactive puncta increased to reach a high level at P21 and onwards (Fig. 8*B*). At these stages, the immunoreactivity was no longer associated with the neuron cell bodies but consisted of puncta surrounding the neurons (Fig. 8*D*). To investigate whether these immunoreactive puncta corresponded to pre- or postsynaptic profiles, double labelling experiments were carried out with anti-mGluR1α antibodies and anti-synaptophysin antibodies, that identify presynaptic terminals. We observed mGluR1α and synaptophysin in neighbouring elements with no colocalization (Fig. 8*D*) suggesting that mGluR1α is localized postsynaptically.

Electron microscopic observations at P6 revealed a very light immunoperoxydase reaction product mainly confined to rare neuron cell bodies and dendrites. In neuron cell bodies, labelling was mainly distributed on plasma membranes and more intensely at the level of the postsynaptic densities (Fig. 8*E*). Immunoperoxydase reaction product was also diffusely distributed in some large dendrites and presented rarely a dense immunolabelling on postsynaptic densities (Fig. 8*F*). At P21, a remarkable feature was the high number of labelled dendritic profiles in comparison with P6. Dendritic profiles were immunoreactive and presented numerous labelled postsynaptic membrane specializations, with a high concentration of labelling opposite to axon terminals (Fig. 8*G*). At P6 and P21 no labelling was found in presynaptic elements, glial cells or glial processes.

mGluR5. During the first week of development, a high density of mGluR5 immunoreactive neurons was present in the vMVN. Most of the labelled neurons were large; however, some small neurons was also immunoreactive (Fig. 9*A* and *C*). Furthermore, a dense labelling of immunoreactive profiles was evident between and around the neuronal cell bodies (Fig. 9*C*). This staining pattern persisted up to P14. From the end of the second week, the most prominent feature was a strong decrease of this dense mGluR5 immunoreactivity to a very faint and diffuse staining at P21 (Fig. 9*B*). Neuronal somas were no longer immunoreactive. To investigate whether the immunoreactivity observed corresponded to the neuronal or glial compartment, double labelling experiments were carried out using antibodies against mGluR5 and antibodies against GFAP, that identifies astrocytic cells

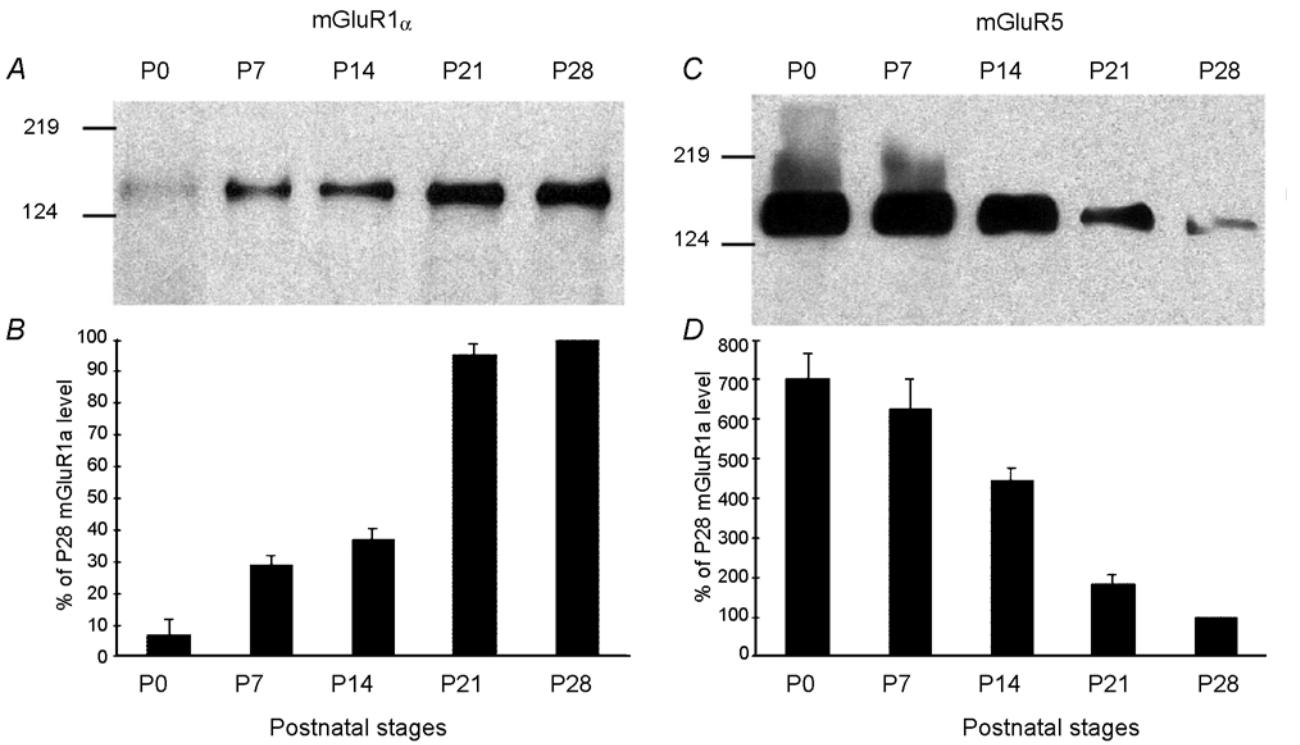

Figure 7. Western blot analysis of mGluR1α and mGluR5 expression in the VN during postnatal development (P0 to P28)

Protein extracts from rat microdissected VN at different postnatal (P) days were collected and analysed for mGluR1α (*A*) and mGluR5 (*C*) expression by Western blot. Note the opposite trend of the changes for mGluR1α and mGluR5 during VN development (*B* and *D*). Data are expressed according to developmental stage (P). The optical density of mGluR subunits for each stage is normalized as a percentage *versus* the P28 value of mGluR expression (100 %). Each data point represents the average value from five experiments. Molecular weight markers are shown on the left.

and processes. At P21, mGluR5 was colocalized with GFAP in numerous profiles (Fig. 9*D*).

Electron microscopy observations at P6 identified immunoperoxydase-labelled profiles mainly localized in dendrites and neuron cell bodies. As observed using confocal microscopy, many neuron cell bodies presented immunoperoxydase labelling (Fig. 9*E*). This labelling was mainly localized around the endoplasmic reticulum and

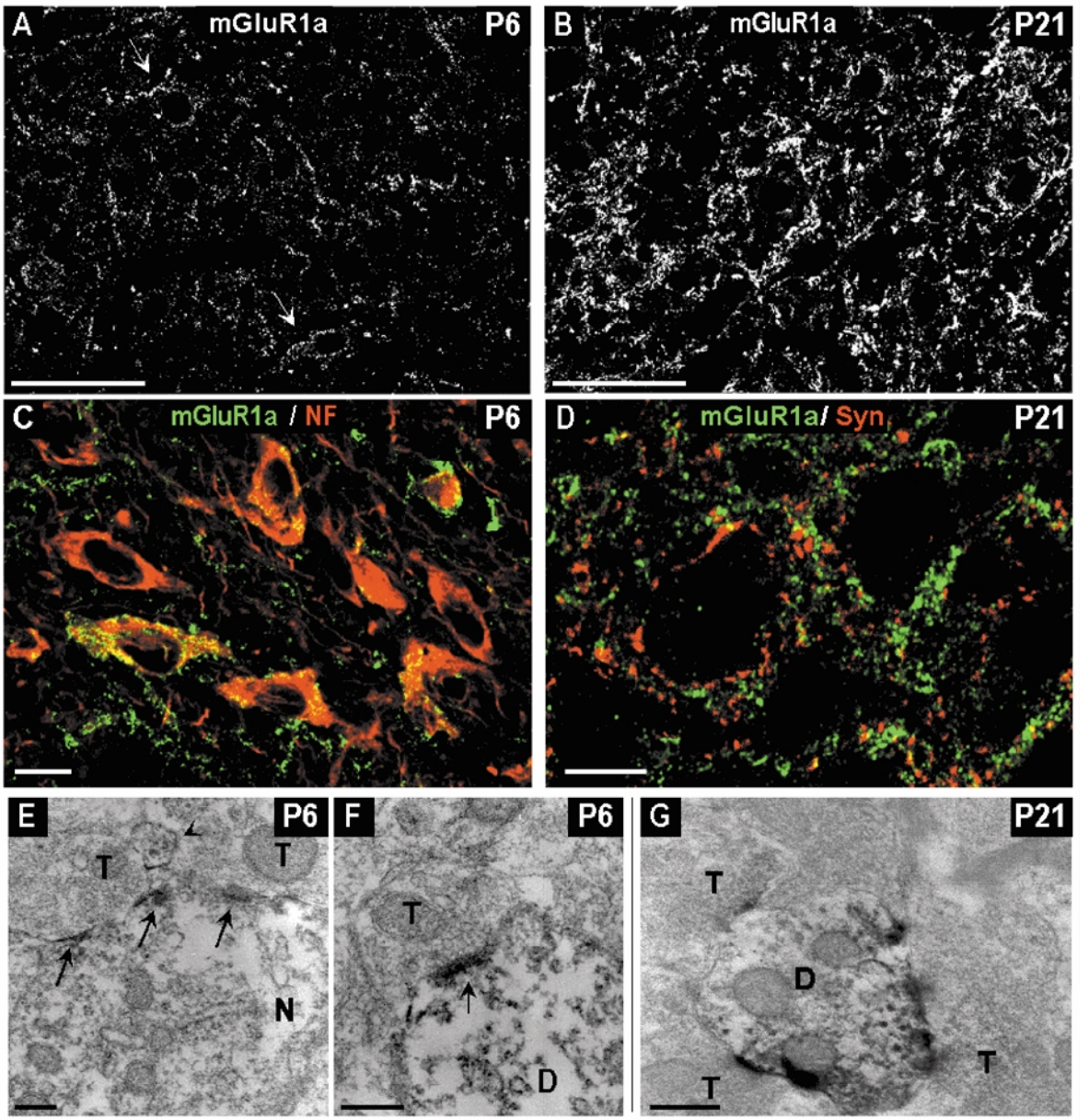

Figure 8. Distribution of mGluR1α immunoreactivity in the developing vMVN visualized by confocal microscopy immunofluorescence and electron microscopy immunoperoxidase staining

A, area of vMVN exhibiting very sparse immunoreactive puncta at P6. Arrows show immunoreactive puncta in neuronal cell bodies. *B*, high density of immunoreactive puncta on P21. *C*, colocalization of anti-mGluR1α (green) and anti-NF (red) antibodies in neurons, at P6. *D*, double labelling with anti-mGluR1α (green) and anti-synaptophysin (red) antibodies did not show any colocalization in the vMVN. Note the closeness of the two markers at P21. Scale bars, 50 μm (*A* and *B*) and 10 μm (*C* and *D*). *E*, in an immunoreactive neuron (N) peroxidase immunoreaction products are mainly concentrated and localized along the postsynaptic membrane specializations (arrows) opposed to two unlabelled axonal terminals (T) at P6. Arrowhead indicates a small labelled dendrite. *F*, strongly immunoreactive postsynaptic density (arrow) in a labelled dendrite (D) at P6. *G*, immunoreactive dendrite in contacted with three unlabelled axonal terminals at P21. Scale bars, 200 nm (*E* and *F*) and 500 nm (*G*).

Journal of Physiology

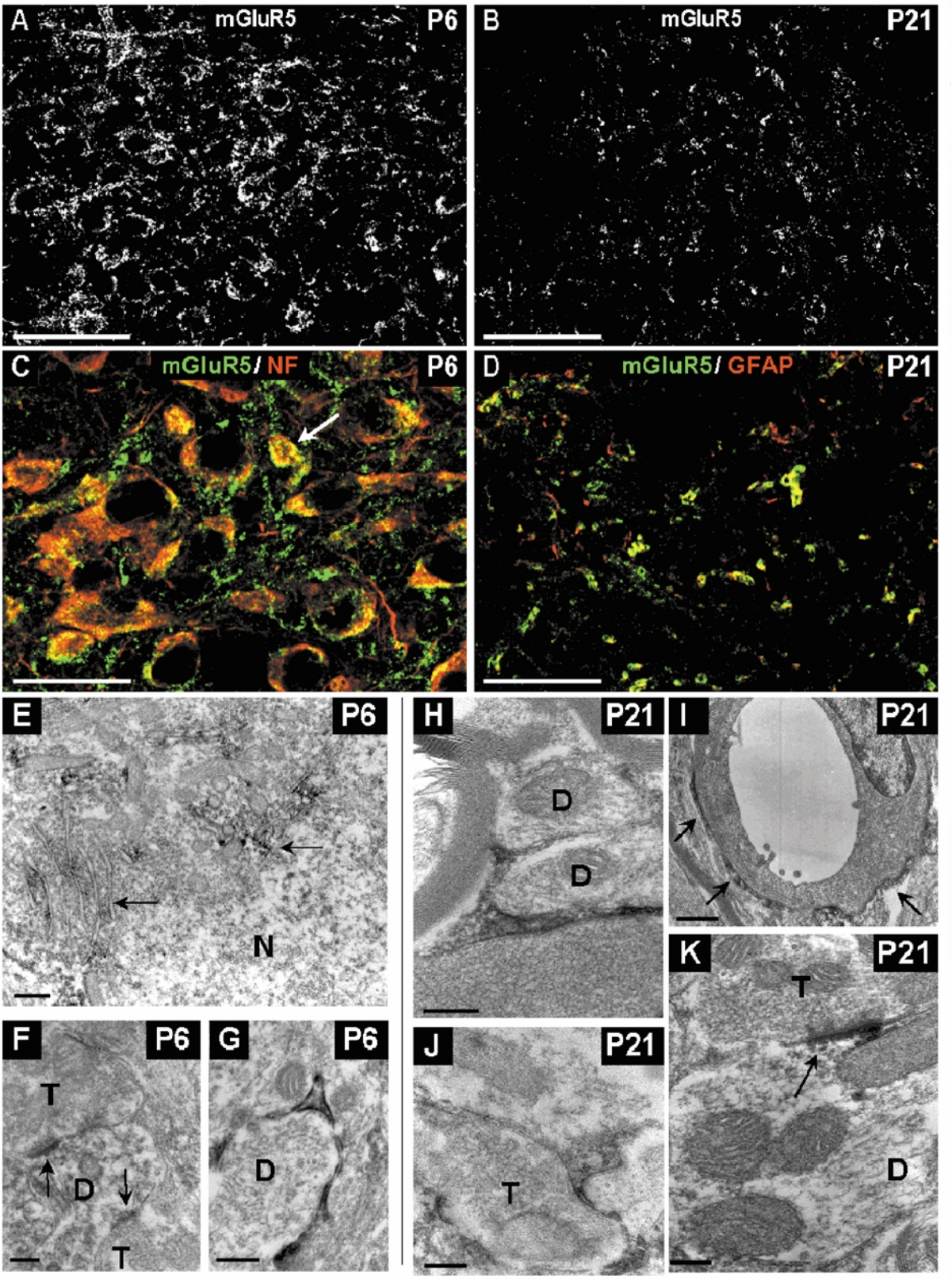

Figure 9. Distribution of mGluR5 immunoreactivity in the developing vMVN visualized by confocal microscopy immunofluorescence and electron microscopy immunoperoxidase staining

A, area of vMVN exhibiting a very high density of staining at P6. Note also the numerous mGluR5 immunoreactive neurons. *B*, sparse immunoreactive puncta at P21. *C*, colocalization of anti-mGluR5 (green) and anti-NF (red) antibodies in neurons at P6. All large neurons express mGluR5 but rare small

Golgi apparatus. A few postsynaptic dendritic profiles exhibited immunoreaction product particularly concentrated at postsynaptic densities (Fig. 9*F*). In addition, at P6, labelled glial cells and processes occupying the narrow spaces between neuronal compartments or ensheathing dendrites were observed (Fig. 9*G*). At P21, ultrastructural observations confirmed the extensive distribution of mGluR5 immunoreactivity in glial processes (Fig. 9*H–J*). Intensely immunostained thin processes of astrocytes ensheathed dendritic profiles (Fig. 9*H*) or axon terminals (Fig. 9*J*). Immunoreaction was also observed in astrocytic processes around capillary walls (Fig 9*I*). Rare postsynaptic dendritic profiles exhibited immunoreaction product (Fig. 9*K*). At P6 and P21 no labelling was found at presynaptic localizations in axon terminals.

DISCUSSION

Our results show that during a critical period of postnatal development (P6–P21), neurons in the vMVN undergo marked modifications in their plastic capability. During the same period, important changes in the mGluR1 and mGluR5 expression and distribution were observed in the vMVN.

Changes in the effects of HFS during postnatal development of the vMVN

Electrophysiological results show that in the first stages of development, HFS of the primary vestibular afferents is not able to induce LTP, which is a consistent phenomenon in the adult vMVN (Capocchi *et al.* 1992; Grassi *et al.* 1996; Grassi & Pettorossi, 2001); however, it provokes LTD, which is never observed in the adult vMVN as a primary mechanism (Capocchi *et al.* 1992; Grassi *et al.* 1996; Grassi & Pettorossi, 2001). It could be suspected that a depression in very young animals results from a deficit of synaptic transmission because of the immaturity of vestibular afferent fibres, which are not yet able to follow HFS. However, the occurrence of LTP when HFS was delivered during blockade of mGluR5 and $GABA_A$ receptors allows us to consider the HFS-induced depression as a true LTD. In addition, the field potential P wave, which represents the afferent volley, was not reduced by HFS. We have demonstrated that LTD does not depend on NMDA receptors, as it was not prevented by AP-5, the NMDA receptor antagonist. HFS-dependent LTD, which does not involve NMDA receptors, has also been demonstrated in other brain structures during development (Artola & Singer, 1993; Battistin & Cherubini, 1994). Conversely, LTD requires activation of mGluR5, a subtype of group I mGluRs, as it was blocked by MPEP, the non-competitive inhibitor of mGluR5. In the adult, mGluR5 is no longer able to induce LTD, but it still maintains an inhibitory role to enhance the threshold for LTP induction (Grassi *et al.* 2002).

In the vMVN, the probability of inducing LTD progressively decreased throughout development, while that of LTP increased, reaching its maximal value at about the end of the third postnatal week. The rise time of LTP was longer during development, and reached its adult value only at the end of the third postnatal week. Like in the adult (Capocchi *et al.* 1992, Grassi *et al.* 2002), LTP depends on the NMDA receptor and mGluR1 activation, as both AP-5 and the mGluR1 antagonist, CPCCOEt, impeded it.

We cannot exclude the possibility that other neurotransmitters and circuits, as well as their developmental changes, may influence the presence of LTD and its gradual disappearance during postnatal development. In particular, it is important to consider the GABAergic circuit, which plays a major inhibitory role in VN. Even though GABA does not affect basal responses and the long-term effect of HFS in the adult vMVN, we found that the block of $GABA_A$ receptors completely prevented HFS-dependent LTD, without affecting basal responses, in the early stages of development. This suggests that the GABA circuit mediates HFS-dependent LTD. The different influence of GABA in young and adult MVN might be due to a remodelling of the vestibular GABAergic circuit during development.

Therefore, we suggest that the induction of LTD, at early stages, requires the activation of both mGluR5 and the feed-forward GABAergic interneurons. In fact, the over activation of the GABAergic circuit, by lowering the excitability of secondary vestibular neurons, would facilitate the induction of LTD, which is mediated by mGluR5. We advance different hypotheses to interpret the interaction between mGluR5 and $GABA_A$ receptors. First, mGluR5 could be indirectly responsible for LTD, as it induces LTP on inhibitory GABAergic interneurons.

neurons (arrow) are also labelled. *D*, double labelling with GFAP (red) and mGluR5 (green) antibodies shows a colocalization in the glial cells of the vMVN. Scale bars, 50 μm (*A* and *B*) and 25 μm (*C* and *D*). *E*, thin small accumulations of immunoreaction product associated with rough endoplasmic reticulum and Golgi apparatus (arrows) in the cytoplasm of the neuron at P6. *F*, mGluR5-labelled postsynaptic densities (arrows) in a dendritic profile opposing two axonal terminals (T). *G*, immunoreactive glial processes ensheathing an unlabelled dendrite (D) at P6. *H*, immunoreactive glial processes ensheathing unlabelled dendrites at P21. *I*, immunoreactive glial processes (arrows) around the wall of a capillary. *J*, labelled glial processes enwrapping an unlabelled axonal terminal. *K*, strongly immunoreactive postsynaptic density opposed to unlabelled axonal terminal at P21. Scale bars, 500 nm (*A* and *E*) and 200 nm (*B*, *C*, *D*, *G* and *F*).

However, this seems unlikely because mGluR5 is mostly localised on the secondary vestibular neurons in our anatomical study. Second, mGluR5 could have a facilitatory influence at the level of the glutamatergic synapse of vestibular secondary neurons, and its activation may induce LTP or LTD depending on the GABAergic activation, which reverses the polarity of the long-term effect. However, the induction of LTP during blockade of mGluR5, seems to exclude this possibility. Therefore, we favour a third hypothesis, that mGluR5 directly mediates LTD, but GABA is required to depress the excitability of the neuron and allow LTD.

Changes in expression and distribution of mGluR1 during postnatal development of vMVN

In the vMVN, the most important change for mGluR1 was the progressive increase of its expression during postnatal development. *In situ* hybridization is limited to a relatively low spatial and quantitative resolution and did not provide convincing information on the expression and subcellular distribution of the protein. The Western blots and immunocytochemical results were precise and consistent with the mGluR1 mRNA variations: there was very little mGluR1α protein at birth and it increased gradually from the end of the first week to P21, when adult levels were reached. A progressive increase in mGluR1 expression has been also observed in other brain regions during postnatal development (Catania *et al.* 1994; Casabona *et al.* 1997) and it has been suggested that while the less expressed receptors in the first development stages might modulate morphogenesis and synaptogenesis, they are involved in the transduction of glutamate signals in mature neuronal circuits (Catania *et al.* 1994).

Confocal and electron microscopic analyses demonstrated that mGluR1α was exclusively localized to the neuronal compartment and identified differences in its subcellular localization during development of vMVN . At P6, the faint expression of mGluR1α occurred mainly in a few neuronal cell bodies, while rare postsynaptic membrane sites were immunoreactive. After the second week, the expression of mGluR1α increased. Double labelling studies with synaptophysin, a marker of presynaptic sites, support the presence of mGluR1α restricted to postsynaptic sites. Our electron microscopic studies definitively showed that mGluR1α had a postsynaptic localization with a high concentration at the postsynaptic membrane specializations, in numerous dendritic profiles of the mature vMVN. Other studies demonstrated developmental changes in the distribution of mGluR1α (Liu *et al.* 1998; Lopez-Bendito *et al.* 2001), which parallel the increase of synaptic activity (Zirpel *et al.* 2000) and their main localization at postsynaptic level in the adult CNS (Baude *et al.* 1993; Lujan *et al.* 1996).

Changes in expression and distribution of mGluR5 during postnatal development of vMVN

In the vMVN, the most important change for mGluR5 was the drastic decrease of its expression during postnatal development. In accordance with the *in situ* hybridization results, Western blot and immunocytochemical analyses revealed a strong decrease of mGluR5 staining density during vMVN development. These changes have been also observed in other brain regions during postnatal development (Catania *et al.* 1994; Romano *et al.* 1996; Casabona *et al.* 1997), suggesting a functional role of mGluR5 during synaptogenesis and maintenance of adult synapses.

A second important developmental change in mGluR5 expression concerned its distribution first mainly in neuronal compartments, then mainly in glia. Indeed, at the youngest stages, mGluR5 was mainly found in the large neuronal cell bodies, which in this area are known as secondary vestibular neurons. However, some small neurons also expressed mGluR5 which may represent GABAergic interneurons (Walberg *et al.* 1990). At this stage, electron microscopic observations showed that mGluR5 labelled postsynaptic dendrites with a high concentration at the postsynaptic membrane specializations, while at older stages, their main localization was in glial cells and processes. Ultrastructural studies have shown that mGluR5 may be localized postsynaptically in various brain regions (Liu *et al.* 1998; Lopez-Bendito *et al.* 2001), but a more diffuse localization in presynaptic terminals and glia has been reported (Romano *et al.* 1995; 1996). It has been shown that glial cells express both ionotropic and metabotropic glutamate receptors, which are relevant to neuron–glia signalling both in developing and mature animals (Vernadakis, 1996; Gallo & Ghiani, 2000). During maturation of the excitatory synapses, astrocytic elements ensheathing the synaptic contacts have been observed in different networks (Liu *et al.* 1998) and are sensitive detectors of changes in extracellular glutamate levels and synaptic strength (Diamond *et al.* 1998). Because mGluR5 are involved in astrocyte activities (Balazs *et al.* 1997), their association with astrocytic processes in vMVN suggest an important role of these receptors in maintaining glutamate levels within the physiological range in the synaptic environment.

Variations of patterns of mGluR and plastic capability of the vMVN during postnatal development

Our anatomical and electrophysiological results suggest that the increase in the occurrence of LTP and decrease of LTD during postnatal development may be related to a progressive maturation of receptors facilitating synaptic responses and a reduction of inhibitory ones. In fact, the

expressions of facilitatory receptors, AMPA, NR2 , that is a group of NMDA subunits (Sans *et al.* 2000) and mGluR1 (present study), show a progressive increase which parallels that of LTP, while that of mGluR5, which plays an inhibitory role on synaptic transmission (Grassi *et al.* 2002), shows a decrease which parallels that of LTD. During development, the coexistence of facilitatory and inhibitory receptors suggests that LTD continues to provide a contrast against the emerging LTP. In fact, the LTP rise time is slowed and, in the presence of the mGluR5 antagonist, MPEP, LTP appeared more frequently showing a faster rise time, at all the ages. To explain the developmental change of LTP rise time, we should take into consideration that, as shown in our previous studies, vestibular LTP is the result of a positive feedback, which is triggered by an initial postsynaptic potentiation, and leads to a progressive increase of glutamate release by retrograde messengers (platelet-activating factor and nitric oxide) (Grassi *et al.* 1998*a*, 1999; Grassi & Petorossi, 2000). Therefore, it is possible that the inhibitory events mediated by mGluR5 and $GABA_A$ receptors, interfere at some level of this positive feedback causing the slowing of LTP building up.

As to the relation between the effect of mGluR5 activation and the amount of receptor expression, it seems that the decrease of mGluR5 distribution is accompanied by a decrease of its inhibitory efficacy. In fact, at the early stages of development, mGluR5 activation seems to be strong enough to induce LTD in the presence of GABAergic activity, while, later on, it is only able to enhance the threshold for LTP and impede potentiation during the normal synaptic transmission (Grassi *et al.* 2002). The reduction of mGluR5 inhibitory efficacy is not questioned by the fact that MPEP is able to induce LTP in the adult, but not in the early stages. In fact, the different effect of MPEP can be attributable to the full efficacy of facilitatory mechanisms and the higher spontaneous release of glutamate, which is present in the adult, but not in the early stages of development. A similar relation between activation effects and amount of receptor expression during development, could be shown for mGluR1, as the occurrence of LTP increases with the expression of this receptor, and it has been shown to play a key role in LTP in the adult (Grassi *et al.* 2002). Even though mGluR1 is necessary for induction of LTP at early stages, while it only mediates the full expression of LTP in the adult, its apparent major facilitatory role in the early stages of development is probably due to the low expression of all the other facilitatory receptors (see NMDA receptor expression) at this age, so that mGluR1 activation is crucial for inducing LTP.

As suggested in other systems, the induction of LTD in developing VN might be important for refining the strength of synaptic connections (Artola & Singer, 1993; Katz & Shatz, 1996; Lo & Mize, 2000). One can suggest that depression of precocious or over-activated synapses may be useful for making their efficacy similar to that of late or under-activated ones. Of interest, the sudden change in the LTD frequency occurred at the time of eye opening, about the end of the second postnatal week. This inhibitory control will remain until the visual experience becomes available and contributes to the final organization of vestibulo-ocular reflex (VOR) circuitry. It is interesting that only when the error signal provided by visual input is available, vestibular synapses can fully express LTP, a finding suggesting that LTP is necessary for establishing the correct spatial connections in the VOR circuitry and consolidating the appropriate connection. In addition, LTP might be also useful for maturation of MVN neuron excitability (Dutia *et al.* 1995; Johnston & Dutia, 1996; Dutia & Johnston, 1998; Murphy & du Lac, 2001).

In conclusion, our results show that there is a change in the plasticity of vestibular synapses during development, consisting in a shift from LTD to LTP. This suggests that synaptic plasticity in the brain is not a fixed property but can change from the birth to adulthood, presumably to sustain distinct developmental and memory-related functions. The shift from LTD to LTP is accompanied by a significant modification of the expression of inhibitory and facilitatory glutamate receptors, suggesting that this change may be one of the factors responsible for the shift from LTD to LTP. Even though other changes in vestibular network may be implied in the LTD–LTP shift, we think that the influence of the mGluR antagonists as well as the correlation between the changes of the mGluR expression and long-term effects, may provide evidence for a role of mGluRs in the developmental changes of vestibular synaptic plasticity.

REFERENCES

Artola A & Singer W (1993). Long-term depression of excitatory synaptic transmission and its relationship to long-term potentiation. *Trends Neurosci* **16**, 480–487.

Balazs R, Miller S, Romano C, De Vries A, Chun Y & Cotman CW (1997). Metabotropic glutamate receptor mGluR5 in astrocytes: pharmacological properties and agonist regulation. *J Neurochem* **69**, 151–163.

Battistin T & Cherubini E (1994). Developmental shift from long-term depression to long term potentiation at the mossy fiber synapse in the rat hippocampus. *Eur J Neurosci* **6**, 1750–1755.

Baude A, Nusser Z, Roberts JD, Mulvihill E, Micilhinney RA & Somogyi P (1993). The metabotropic glutamate receptor (mGluR1 alpha) is concentrated at perisynaptic membrane of neuronal subpopulations as detected by immunogold reaction. *Neuron* **11**, 771–787.

Capocchi G, Della Torre G, Grassi S, Pettorossi VE & Zampolini M (1992). NMDA-mediated long term modulation of electrically evoked field potentials in the rat medial vestibular nuclei. *Exp Brain Res* **90**, 546–550.

Casabona G, Knopfel T, Kuhn R, Gasparini F, Baumann P, Sortino MA, Copani A & Nicoletti F (1997). Expression and coupling to polyphosphoinositide hydrolysis of group I metabotropic glutamate receptors in early postnatal and adult rat brain. *Eur J Neurosci* **9**, 12–17.

Catania MV, Bellomo M, Di Giorgi-Gerevini V, Seminara G, Giuffrida R, Romeo R, De Blasi A & Nicoletti F (2001). Endogenous activation of group I metabotropic glutamate receptors is required for differentiation and survival of cerebellar Purkinje cells. *J Neurosci* **21**, 7664–7673.

Catania MV, Landwehrmeyer GB, Testa CM, Standaert DG, Penney JB Jr & Young AB (1994). Metabotropic glutamate receptors are differentially regulated during development. *Neuroscience* **61**, 481–495.

Conn PJ & Pin JP (1997). Pharmacology and functions of metabotropic glutamate receptors. *Annu Rev Pharmacol* **37**, 205–237.

Curthoys IS (1982). Postnatal developmental changes in the response of rat primary horizontal semicircular canal neurons to sinusoidal angular accelerations. *Exp Brain Res* **47**, 295–300.

Diamond JS, Bergles DE & Jahr CE (1998). Glutamate release monitored with astrocyte transporter currents during LTP. *Neuron* **21**, 425–433.

Dudek SM & Bear MF (1993). Bidirectional long-term modification of synaptic effectiveness in the adult and immature hippocampus. *J Neurosci* **13**, 2910–2918.

Dutia MB & Johnston AR (1998). Development of action potentials and apamin-sensitive after-potentials in mouse vestibular nucleus neurones. *Exp Brain Res* **118**, 148–154.

Dutia MB, Lotto RB & Johnston AR (1995). Post-natal development of tonic activity and membrane excitability in mouse medial vestibular nucleus neurones. *Acta Otolaryngol Suppl* **502**, 101–104.

Fotuhi M, Standaert DG, Testa CM, Penney JB Jr & Young AB (1994). Differential expression of metabotropic glutamate receptors in the hippocampus and entorhinal cortex of the rat. *Brain Res Mol Brain Res* **21**, 283–292.

Gallo V & Ghiani CA (2000). Glutamate receptors in glia: new cells, new inputs and new functions. *Trends Pharmacol Sci* **21**, 252–258.

Gasparini F, Lingenhöhl K, Stoehr N, Flor PJ, Heinrich M, Vranesic I, Biollaz M, Allgeier H, Heckendorn R, Urwyler S, Varney MA, Johnson EC, Hess SD, Rao SP, Sacaan AI, Santori EM, Veliçelibi G & Kuhn R (1999). 2-Methyl-6-phenylethynyl)-pyridine (MPEP), a potent, selective, and systemically active mGlu5 receptor antagonist. *Neuropharmacology* **38**, 1493–1503.

Grassi S, Della Torre G, Capocchi G, Zampolini M & Pettorossi VE (1995). The role of GABA in NMDA-dependent long term depression (LTD) of rat medial vestibular nuclei. *Brain Res* **699**, 183–191.

Grassi S, Francescangeli E, Goracci F & Pettorossi VE (1998*a*). Role of platelet-activating factor in long term potentiation of the rat medial vestibular nuclei. *J Neurophysiol* **79**, 3266–3271.

Grassi S, Francescangeli E, Goracci F & Pettorossi VE (1999). Platelet activating factor and group I metabotropic glutamate receptors interact for full development and maintenance of long term potentiation in the rat medial vestibular nuclei. *Neuroscience* **94**, 549–559.

Grassi S, Frondaroli A & Pettorossi VE. (2002). Different metabotropic glutamate receptors play opposite roles in synaptic plasticity of the rat medial vestibular nuclei. *J Physiol* **543**, 795–806.

Grassi S, Malfagia C & Pettorossi VE (1998*b*). Effects of metabotropic glutamate receptor block on the synaptic transmission and plasticity in the rat medial vestibular nuclei. *Neuroscience* **87**, 159–169.

Grassi S & Pettorossi VE (2000). Role of nitric oxide in long-term potentiation of the rat medial vestibular nuclei. *Neuroscience* **101**, 157–164.

Grassi S & Pettorossi VE (2001). Synaptic plasticity in the medial vestibular nuclei: role of glutamate receptors and retrograde messengers in rat brainstem slices. *Prog Neurobiol* **64**, 527–553.

Grassi S, Pettorossi VE & Zampolini M (1996). Low frequency stimulation cancels the high frequency-induced long lasting effects in the rat medial vestibular nuclei. *J Neurosci* **16**, 3373–3380.

Heywood P, Pujol R & Hilding D (1973). Early synapse formation in vestibular system of fetal guinea pig. *Brain Res* **51**, 337–339.

Johnston AR & Dutia MB (1996). Postnatal development of spontaneous tonic activity in mouse medial vestibular nucleus neurones. *Neurosci Lett* **219**, 17–20.

Karhunen E (1973). Postnatal development of the lateral vestibular nucleus (Deiter's nucleus) of the rat. *Acta Otolaryngol* **313**, 1–87.

Katz LC & Shatz CJ (1996). Synaptic activity and the construction of cortical circuits. *Science* **274**, 1133–1138.

Kirkwood A, Lee HK & Bear MF (1995). Co-regulation of long-term potentiation and experience-dependent plasticity in visual cortex by age and experience. *Nature* **375**, 328–331.

Lannou J, Precht W & Cazin L (1979). The postnatal development of functional properties of central vestibular neurons in the rat. *Brain Res* **175**, 219–232.

Litschig S, Gasparini F, Ruegg D, Stoehr N, Flor PJ, Vranesic I, Prézeau L, Pin JP, Thomsen C & Kuhn R (1999). CPCCOEt, a non-competitive metabotropic glutamate receptor 1 antagonist, inhibits receptor signalling without affecting glutamate binding. *Mol Pharmacol* **55**, 453–461.

Liu XB, Munoz A & Jones EG (1998). Changes in subcellular localization of metabotropic glutamate receptor subtypes during postnatal development of mouse thalamus. *J Comp Neurol* **395**, 450–465.

Lo FS & Mize RR (2000). Synaptic regulation of L-type Ca^{2+} channel activity and long-term depression during refinement of the retinocollicular pathway in developing rodent superior colliculus. *J Neurosci* **20**, RC58.

Lo FS & Mize RR (2002). Properties of LTD and LTP of retinocollicular synaptic transmission in the developing rat superior collicus. *Eur J Neurosci* **15**, 1421–1432.

Lopez-Bendito G, Shigemoto R, Lujan R & Juiz JM (2001). Developmental changes in the localisation of the mGluR1alpha subtype of metabotropic glutamate receptors in Purkinje cells. *Neuroscience* **105**, 413–429.

Lujan R, Nusser Z, Roberts JD, Shigemoto R & Somogyi P (1996). Perisynaptic location of metabotropic glutamate receptors mGluR1 and mGluR5 on dendrites and dendritic spines in the rat hippocampus. *Eur J Neurosci* **8**, 1488–1500.

Mehler WR & Rubertone JA (1985). Anatomy of the vestibular nucleus complex. In *The Rat Nervous System*, vol 2. *Hindbrain and Spinal Cord*, ed. Paxinos, G., pp. 185–219. Academic Press, New York.

Murphy GJ & Du Lac S (2001). Postnatal development of spike generation in rat medial vestibular nucleus neurons. *J Neurophysiol* **85**, 1899–1906.

Paxinos G & Watson C (1986). *The Rat Brain in Sterotaxic Coordinates*. Academic Press, Sydney.

Puyal J, Devau G, Venteo S, Sans N & Raymond J (2002). Calcium-binding proteins map the postnatal development of rat vestibular nuclei and their vestibular and cerebellar projections. *J Comp Neurol* **451**, 374–391.

Reid SN, Romano C, Hughes T & Daw NW (1995). Immunohistochemical study of two phosphoinositide-linked metabotropic glutamate receptors (mGluR1 alpha and mGluR5) in the cat visual cortex before, during, and after the peak of the critical period for eye-specific connections. *J Comp Neurol* **355**, 470–477.

Romano C, Sesma MA, McDonald CT, O'Malley K, Van Den Pol AN & Olney JW (1995). Distribution of metabotropic glutamate receptor mGluR5 immunoreactivity in rat brain. *J Comp Neurol* **355**, 455–469.

Romano C, Van Den Pol AN & O'Malley KL (1996). Enhanced early developmental expression of the metabotropic glutamate receptor mGluR5 in rat brain: protein, mRNA splice variations, and regional distribution. *J Comp Neurol* **367**, 403–412.

Sans NA, Montcouquiol ME & Raymond J (2000). Postnatal development changes in AMPA and NMDA receptors in the rat vestibular nuclei. *Brain Res Dev Brain Res* **123**, 41–52.

Vernadakis A (1996). Glia-neuron intercommunications and synaptic plasticity. *Prog Neurobiol* **49**, 185–214.

Walberg F, Ottersen OP & Rinvik E (1990). GABA, glycine, aspartate, glutamate and taurine in the vestibular nuclei: an immunocytochemical investigation in the cat. *Exp Brain Res* **79**, 547–563.

Zirpel L, Janowiak MA, Taylor DA & Parks TN (2000). Developmental changes in metabotropic glutamate receptor-mediated calcium homeostasis. *J Comp Neurol* **421**, 95–106.

Acknowledgements

This research was supported by a grant from the Italian Ministry of University and Scientific Research. We wish to thank D. Bambagioni and S. Ventéo for their excellent technical assistance. We wish to thank Nathalie Sans for research assistance and *in situ* hybridization illustrations. We thank Dr G. Dayanithi for critical revision of the manuscript.